CILAMCE 2017
Florianópolis - Santa Catarina - Brazil

MODELING FLUID-FILLED CYLINDRICAL SHELLS WITH WAVE FINITE ELEMENTS

R. W. O. Sousa

raystonsousa@gmail.com

Departament of Computational Mechanics, University of Campinas-UNICAMP

Rua Mendeleyev 200, CEP 13083-860, Campinas, SP, Brazil

J.-M. Mencik

jean-mathieu.mencik@insa-cvl.fr

INSA Centre Val de Loire, Campus de Blois, Rue de la Chocolaterie, 41000 Blois, France

J. M. C. Dos Santos

zema@fem.unicamp.br

Departament of Computational Mechanics - University of Campinas-UNICAMP

Rua Mendeleyev 200, CEP 13083-860, Campinas, SP, Brazil

Abstract. *The wave finite element (WFE) method is applied to analyze the guided wave propagation in fluid-filled cylindrical shells. In this study, the cylindrical shells are assumed to be linear elastic and modeled with 2D flat shell elements, while the inner fluids are assumed to be acoustic and modeled with 3D linear elements. A periodic finite element (FE) mesh assumption is used which enables the description of a whole fluid-filled cylindrical shell in terms of identical subsystems which are composed of structure parts and fluid parts, and which are assembled together along a straight direction. By considering the FE model of a subsystem, a transfer matrix relation can be derived which links the kinematic/mechanical quantities between the right and left cross-sections. Also, the eigenvalues and eigenvectors of the transfer matrix provides the so-called wave modes, i.e., the wave parameters/wave numbers and the wave shapes. Besides, the WFE method is applied to compute the vibroacoustic responses of fluid-filled cylindrical shells of finite length and whose left and right ends are subject to prescribed vectors of displacements/pressures and elastic/acoustic forces. Several simulations are performed which highlight the relevance of the WFE method.*

Keywords: *Wave propagation, Fluid-filled cylindrical shells, Wave finite element method, Vibroacoustic response*

1 INTRODUCTION

Cylindrical shells filled with acoustic fluids — e.g., gas pipelines or exhaust pipes — are frequently encountered in many applications such as Non Destructive Testing (NDT) and the design of exhaust mufflers. Nowadays, a large amount of analytical formulations have been developed which analyze the guided elasto-acoustic wave propagation along these systems (Kumar, 1972; Kumar and Stephens, 1972; Sinha et al., 1992; Fuller and Fahy, 1982). Despite this, those wave propagation mechanisms are still not well understood at high frequencies, especially for predicting the complex energy conversion phenomena which occur between the acoustic and elastic wave motions. As a second drawback, the analytical theories are fairly limited to the analysis of homogeneous systems with simple geometry (Mencik and Ichchou, 2007). To circumvent this problem, the Finite Element (FE) method can be used. While the FE method is well suited to model elasto-acoustic waveguides with arbitrary-shaped cross-sections, it requires dense mesh discretization to accurately describe the system behavior, which penalizes the computational efficiency of the method. On the other hand, the Wave Finite Element (WFE) method can be considered, especially for periodic systems with many degrees of freedom (DOFs) like those involving shell elements. The WFE method constitutes a fast and accurate numerical tool for computing the wave modes in periodic structures, and further their vibroacoustic responses. The WFE method is not constrained to the low frequency range as opposed to the analytical approaches, and provides the same level of accuracy as the FE method. Within the WFE framework, the FE model of a small slice of a whole system is considered and a transfer matrix relation is expressed to link the kinematic/mechanical quantities between the right and left boundaries of this slice. By considering the Bloch's theorem, the so-called wave modes of the periodic system can be computed, which involves assessing the eigenvalues and eigenvectors of the transfer matrix of the slice (Mencik and Ichchou, 2005). The proposed strategy reduces considerably the computational times when compared to the FE method.

So far, several WFE strategies have been proposed to calculate the wave propagation and vibroacoustic response of elasto-acoustic systems. One of the main works was carried out by Mencik and Ichchou (2007) in which a symmetric matrix formulation is considered to assess the wave propagation in fluid-filled periodic structures. Also, Manconi et al. (2009) applied the WFE method to axisymmetric fluid-filled pipes. More recently, the WFE method has been used to investigate the acoustic radiation of fluid-filled elastic pipes (Bhuddi et al., 2015; Gobert and Mencik, 2016). Even though many researches have been conducted on elasto-acoustic systems, only a few of these focus on systems whose elastic part is modeled with shell elements. These shell-based models are supposed to be more relevant compared to the case when the structure part is modeled with linear 3D elements, and provide better accuracy for predicting the wave propagation and vibroacoustic responses at high frequencies. Here lies the motivation of the present work.

In this paper, the WFE method is applied to calculate the wave propagation and vibroacoustic response of cylindrical shells filled with an internal acoustic fluid. The FE modeling of a periodic subsystem is presented first. This FE model is based on the symmetric matrix formulation which consists in using the displacements and velocity potentials as field variables. The proposed WFE-based approach is validated by analyzing the vibroacoustic response of a fluid-filled cylindrical shell of finite length and subject to harmonic acoustic loads. Dispersion curves are assessed and compared with the analytical theory. Additional experiments are made to highlight the relevance of the proposed method in terms of accuracy and CPU time savings, in comparison with the FE method.

2 WFE METHOD

2.1 Subsystem modeling

The WFE method starts by considering the FE model of a slice/subsystem of a periodic system. The system is periodic in the sense that it is composed of identical subsystems, of length d, along a certain straight direction (say z-axis) (Mencik and Ichchou, 2005). The subsystems under concern are made of a structure part which is supposed to be elastic and dissipative, and an inner fluid part consisting in an acoustic fluid which is supposed to be inviscid.

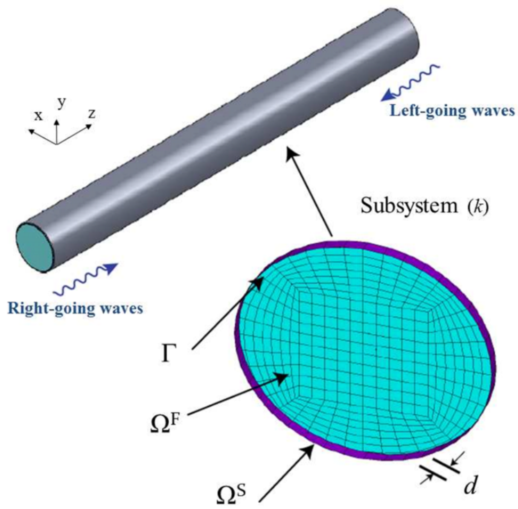

Figure 1: FE model of an elasto-acoustic subsystem.

Consider a subsystem k ($k = 1, ..., N$) as shown in Figure 1. The left and right cross-sections (boundaries) of the subsystem are meshed using the same number n of DOFs. Here, the total number of DOFs on the boundaries is expressed as $n = n^{\mathtt{S}} + n^{\mathtt{F}}$, where $n^{\mathtt{S}}$ and $n^{\mathtt{F}}$ are the numbers of DOFs on the boundaries of the structure part and fluid part, respectively. In the present study, the FE mesh of the subsystem (cf. Figure 1) involves 2D flat shell elements for the structure part (cylindrical shell) and 3D acoustic elements for the fluid part (internal fluid). Hexahedral elements in the fluid volume allow reduce the element count, processing time and memory usage because this model is highly space efficient. In this case, the mesh is mapped with a square inside the circle which allows greater control of the element size.

Structure part. A shell element combines a bending behavior with an "in-plane" (membrane) motion. As the governing equations of a curved shell are quite complex due to the curvature of the middle surface, many alternative strategies have been used as a means of overcoming this problem. One practical approach is the development of flat shell elements that include both in-plane and bending motions by combining a membrane element together with a Kirchhoff-Love plate element (Zienkiewicz and Taylor, 2000; Quek and Liu, 2003). In this framework, a cylindrical shell is meshed with 2D rectangular thin flat shell elements with four nodes and six degrees of freedom (DOFs) per node (i.e., three displacements and three rotations) that incorporate both bending and membrane actions with drilling DOFs (Zienkiewicz and Taylor, 2000; Bathe, 2015). As it turns out, the element stiffness matrix (24×24) and element mass matrix (24×24) of a shell element are expressed as follows (Romero, 2007):

$$\mathbf{K}_e^{\mathtt{S}} = \begin{bmatrix} \mathbf{K}_e^{\mathtt{m}} & \mathbf{0} & \mathbf{0} \\ \mathbf{0} & \mathbf{K}_e^{\mathtt{b}} & \mathbf{0} \\ \mathbf{0} & \mathbf{0} & \mathfrak{K}\mathbf{I} \end{bmatrix}, \tag{1}$$

$$\mathbf{M}_e^{\mathtt{S}} = \begin{bmatrix} \mathbf{M}_e^{\mathtt{m}} & \mathbf{0} & \mathbf{0} \\ \mathbf{0} & \mathbf{M}_e^{\mathtt{b}} & \mathbf{0} \\ \mathbf{0} & \mathbf{0} & \mathfrak{M}\mathbf{I} \end{bmatrix}, \tag{2}$$

where $\mathbf{K}_e^{\mathtt{m}}$ and $\mathbf{M}_e^{\mathtt{m}}$ are, respectively, the 8×8 element stiffness and mass matrices corresponding to the membrane motion; $\mathbf{K}_e^{\mathtt{b}}$ and $\mathbf{M}_e^{\mathtt{b}}$ are, respectively, the 12×12 element stiffness and mass matrices corresponding to the bending motion; finally, $\mathfrak{K}$ and $\mathfrak{M}$ are two approximate coefficients which reflect the rotation DOFs (θ_z) in the element stiffness and mass matrices (Bathe, 2015). As a result, the global stiffness and mass matrices of the structural part are expressed as (Zienkiewicz and Taylor, 2000; Romero, 2007):

$$\mathbf{K}^{\mathtt{S}} = \sum\nolimits_e (\mathbf{L}_e^{\mathtt{S}})^T \mathbf{K}_e^{\mathtt{S}} \mathbf{L}_e^{\mathtt{S}}, \tag{3}$$

$$\mathbf{M}^{\mathtt{S}} = \sum\nolimits_e (\mathbf{L}_e^{\mathtt{S}})^T \mathbf{M}_e^{\mathtt{S}} \mathbf{L}_e^{\mathtt{S}}, \tag{4}$$

where $\mathbf{L}_e^{\mathtt{S}}$ are element localization matrices.

Fluid part. The governing equation of the fluid domain is given by the Helmholtz equation (Morand and Ohayon, 1992):

$$\nabla^2 p + \frac{\omega^2}{c_0^2} p = 0 \quad \text{in}\, \Omega^{\mathtt{F}}, \tag{5}$$

where p is the acoustic pressure of the fluid, ∇^2 is the Laplacian differential operator; ω and c_0 stand for the pulsation and the speed of sound, respectively. The FE model of the fluid part can be obtained by considering the method of Weighted Residuals (Bathe, 2015). In this case, 3D isoparametric elements with eight nodes and one DOF per node (pressure) are considered. Hence, the element acoustic stiffness and mass matrices are expressed as follows (Sandberg and Ohayon, 2009):

$$\mathbf{K}_{e'}^{\mathtt{F}} = \int_{\Omega_f} \left(\nabla \mathbf{N}_{e'}^{\mathtt{F}}\right)^T \nabla \mathbf{N}_{e'}^{\mathtt{F}} dV, \tag{6}$$

$$\mathbf{M}_{e'}^{\mathtt{F}} = \frac{1}{c_0^2} \int_{\Omega_f} \left(\mathbf{N}_{e'}^{\mathtt{F}}\right)^T \mathbf{N}_{e'}^{\mathtt{F}} dV, \tag{7}$$

where $\mathbf{N}_{e'}^{\mathtt{F}}$ is the matrix of shape functions for a 3D linear element. Hence, the global stiffness and mass matrices of the fluid part are obtained as follows:

$$\mathbf{K}^{\mathtt{F}} = \sum\nolimits_{e'} (\mathbf{L}_{e'}^{\mathtt{F}})^T \mathbf{K}_{e'}^{\mathtt{F}} \mathbf{L}_{e'}^{\mathtt{F}}, \tag{8}$$

$$\mathbf{M}^{\mathtt{F}} = \sum\nolimits_{e'} (\mathbf{L}^{\mathtt{F}}_{e'})^T \mathbf{M}^{\mathtt{F}}_{e'} \mathbf{L}^{\mathtt{F}}_{e'}, \tag{9}$$

where $\mathbf{L}^{\mathtt{F}}_{e'}$ are element localization matrices.

Fluid-structure interaction. The coupling conditions between two elements e and e' in the structural and fluid parts are managed by considering a coupling matrix $\mathbf{C}_{\mathbf{ee'}}$ (Sandberg and Ohayon, 2009):

$$\mathbf{C}_{ee'} = \int_{\Gamma_{ee'}} \left(\mathbf{N}^{\mathtt{S}}_{e}\right)^T \mathbf{n}^{\mathtt{F}}_{e'} \mathbf{N}^{\mathtt{F}}_{e'} dS \quad \Rightarrow \quad \mathbf{C} = \sum\nolimits_{e} \sum\nolimits_{e'} (\mathbf{L}^{\mathtt{S}}_{e})^T \mathbf{C}_{ee'} \mathbf{L}^{\mathtt{F}}_{e'}, \tag{10}$$

where $\mathbf{n}^{\mathtt{F}}_{e}$ is the outward unit normal vector at the boundary of the fluid domain, and $\Gamma_{ee'}$ represents the part of the coupling interface between the elements e (structure) and e' (fluid). The coupling is performed by linear interpolation for the displacement and cubic interpolation for the rotations.

By considering the mass, stiffness and coupling matrices of the subsystem, the following unsymmetric formulation $(\mathbf{U}, \mathbf{p})$ can be obtained (Morand and Ohayon, 1992):

$$-\omega^2 \begin{bmatrix} \mathbf{M}^{\mathtt{S}} & \mathbf{0} \\ \rho_0 \mathbf{C}^T & \mathbf{M}^{\mathtt{F}} \end{bmatrix} \begin{pmatrix} \mathbf{U} \\ \mathbf{p} \end{pmatrix} + \begin{bmatrix} \mathbf{K}^{\mathtt{S}} & -\mathbf{C} \\ \mathbf{0} & \mathbf{K}^{\mathtt{F}} \end{bmatrix} \begin{pmatrix} \mathbf{U} \\ \mathbf{p} \end{pmatrix} = \begin{pmatrix} \mathbf{F}^{\mathtt{S}} \\ \mathbf{F}^{\mathtt{F}} \end{pmatrix}, \tag{11}$$

where $\mathbf{U}$ and $\mathbf{p}$ are the vectors of nodal displacements and nodal pressures, respectively; $\mathbf{F}^{\mathtt{S}}$ and $\mathbf{F}^{\mathtt{F}}$ are the structural and acoustic force vectors, respectively; ρ_0 is the fluid density. Mencik and Ichchou (2007) proposed the use of a symmetric matrix formulation based on displacements and velocity potentials as field variables, with a view to expressing a transfer matrix which is symplectic (this provides the usual properties that waves should occur in pairs, i.e., right-going and left-going wave modes). This symmetric matrix formulation is expressed as follows:

$$\mathbf{D}\mathbf{q} = \mathbf{F}, \tag{12}$$

where $\mathbf{q}$ and $\mathbf{F}$ represents the vectors of kinematic variables:

$$\mathbf{q} = \begin{pmatrix} \mathbf{U} \\ \mathbf{\Psi} \end{pmatrix}, \tag{13}$$

$$\mathbf{F} = \begin{pmatrix} \mathbf{F}^{\mathtt{S}} \\ \frac{1}{\mathtt{i}\omega} \mathbf{F}^{\mathtt{F}} \end{pmatrix}, \tag{14}$$

where $\mathbf{\Psi}$ is the vector of velocity potentials defined as $\mathbf{p} = -\mathtt{i}\omega\rho_0\mathbf{\Psi}$. Also, $\mathbf{D}$ represents the dynamic stiffness matrix of the subsystem (Morand and Ohayon, 1992):

$$\mathbf{D} = -\omega^2 \begin{bmatrix} \mathbf{M}^{\mathtt{S}} & \mathbf{0} \\ \mathbf{0} & -\rho_0 \mathbf{M}^{\mathtt{F}} \end{bmatrix} + \mathtt{i}\omega \begin{bmatrix} \mathbf{0} & \rho_0 \mathbf{C} \\ \rho_0 \mathbf{C}^T & \mathbf{0} \end{bmatrix} + \begin{bmatrix} \mathbf{K}^{\mathtt{S}} & \mathbf{0} \\ \mathbf{0} & -\rho_0 \mathbf{K}^{\mathtt{F}} \end{bmatrix}. \tag{15}$$

Notice that the structure part is supposed to be damped with a loss factor η, i.e., the stiffness matrix of the structure part is complex and expressed as $\mathbf{K}^{\mathtt{S}} = \Re\{\mathbf{K}^{\mathtt{S}}\}(1 + \mathtt{i}\eta)$.

2.2 Wave mode computation

Following the WFE framework (Mencik and Ichchou, 2005; Zhong and Williams, 1995), the elasto-acoustic wave modes $(\mu_j, \boldsymbol{\phi}_j)$ are obtained by solving an eigenproblem of the form

$$\mathbf{S}\boldsymbol{\phi}_j = \mu_j \boldsymbol{\phi}_j, \tag{16}$$

where μ_j and $\boldsymbol{\phi}_j$ are the eigenvalues and eigenvectors of $\mathbf{S}$. Here, $\mathbf{S}$ is the transfer matrix of the subsystem (size of $2n \times 2n$) which is symplectic and expressed as

$$\mathbf{S} = \left[\begin{array}{c|c} -\mathbf{D}_{\mathtt{LR}}^{*-1}\mathbf{D}_{\mathtt{LL}}^{*} & -\mathbf{D}_{\mathtt{LR}}^{*-1} \\ \hline \mathbf{D}_{\mathtt{RL}}^{*} - \mathbf{D}_{\mathtt{RR}}^{*}\mathbf{D}_{\mathtt{LR}}^{*-1}\mathbf{D}_{\mathtt{LL}}^{*} & -\mathbf{D}_{\mathtt{RR}}^{*}\mathbf{D}_{\mathtt{LR}}^{*-1} \end{array} \right], \tag{17}$$

in which the subscripts $\mathtt{L}$ and $\mathtt{R}$ refer to the left and right boundaries of the subsystem, and $\mathbf{D}^*$ is the condensed dynamic stiffness matrix of the subsystem, expressed by

$$\mathbf{D}^* = \mathbf{D}_{\mathtt{BB}} - \mathbf{D}_{\mathtt{BI}}\mathbf{D}_{\mathtt{II}}^{-1}\mathbf{D}_{\mathtt{IB}}, \tag{18}$$

where the subscripts $\mathtt{B}$ and $\mathtt{I}$ refer to the boundary DOFs (i.e., those on the left and right cross-sections) and the internal DOFs, respectively. In case of no internal DOFs, one has $\mathbf{D}^* = \mathbf{D}$. The eigenvalues μ_j of the transfer matrix $\mathbf{S}$ have the meaning of propagation constants, expressed as $\mu_j = \mathtt{exp}(-\mathrm{i}\beta_j d)$ where d is the subsystem length and β_j designates the wavenumbers. Also, the eigenvectors $\boldsymbol{\phi}_j$ have the meaning of wave shapes defined as $\boldsymbol{\phi}_j = [(\boldsymbol{\phi}_{\mathtt{q}})_j{}^T (\boldsymbol{\phi}_{\mathtt{F}})_j{}^T]^T$ where, in this case

$$\boldsymbol{\phi}_{\mathtt{q}} = \begin{bmatrix} \boldsymbol{\phi}_{\mathtt{q}}^{\mathtt{S}} \\ \boldsymbol{\phi}_{\mathtt{q}}^{\mathtt{F}} \end{bmatrix}, \tag{19}$$

$$\boldsymbol{\phi}_{\mathtt{F}} = \begin{bmatrix} \boldsymbol{\phi}_{\mathtt{F}}^{\mathtt{S}} \\ \boldsymbol{\phi}_{\mathtt{F}}^{\mathtt{F}} \end{bmatrix}. \tag{20}$$

Here, $\boldsymbol{\phi}_{\mathtt{q}}^{\mathtt{S}}$ and $\boldsymbol{\phi}_{\mathtt{F}}^{\mathtt{S}}$ are associated to the displacements and forces on the boundaries of the structure part, while $\boldsymbol{\phi}_{\mathtt{q}}^{\mathtt{F}}$ and $\boldsymbol{\phi}_{\mathtt{F}}^{\mathtt{F}}$ are associated to the velocity potentials and acoustic forces on the boundaries of the fluid part. Due to the symplectic property of the matrix $\mathbf{S}$, the eigensolutions occur in pairs as $(\mu_j, 1/\mu_j)$, i.e, there exist n right-going wave modes $\{(\mu_j, \boldsymbol{\phi}_j)\}_{j=1,\ldots,n}$ and n left-going wave modes $\{(\mu_j^\star, \boldsymbol{\phi}_j^\star)\}_{j=1,\ldots,n}$, where μ_j with $|\mu_j| < 1$ and $\mu_j^\star = 1/\mu_j$ with $|\mu_j^\star| > 1$. In matrix form, those wave modes are written as:

$$\boldsymbol{\mu} = (\boldsymbol{\mu}^\star)^{-1} = \mathtt{diag}\{\mu_{\mathrm{j}}\}_{j=1,\ldots,n}, \tag{21}$$

$$\boldsymbol{\Phi} = \begin{bmatrix} \boldsymbol{\Phi}_{\mathtt{q}} \\ \boldsymbol{\Phi}_{\mathtt{F}} \end{bmatrix} = \begin{bmatrix} (\boldsymbol{\phi}_{\mathtt{q}})_1 \ldots (\boldsymbol{\phi}_{\mathtt{q}})_n \\ (\boldsymbol{\phi}_{\mathtt{F}})_1 \ldots (\boldsymbol{\phi}_{\mathtt{F}})_n \end{bmatrix}, \tag{22}$$

$$\boldsymbol{\Phi}^\star = \begin{bmatrix} \boldsymbol{\Phi}_{\mathtt{q}}^\star \\ \boldsymbol{\Phi}_{\mathtt{F}}^\star \end{bmatrix} = \begin{bmatrix} (\boldsymbol{\phi}_{\mathtt{q}}^\star)_1 \ldots (\boldsymbol{\phi}_{\mathtt{q}}^\star)_n \\ (\boldsymbol{\phi}_{\mathtt{F}}^\star)_1 \ldots (\boldsymbol{\phi}_{\mathtt{F}}^\star)_n \end{bmatrix}, \tag{23}$$

in which $\mathbf{\Phi}_{\mathrm{q}}$, $\mathbf{\Phi}_{\mathrm{q}}^{\star}$, $\mathbf{\Phi}_{\mathrm{F}}$ and $\mathbf{\Phi}_{\mathrm{F}}^{\star}$ are $n \times n$ matrices partitioned into structure and fluid components. The direct computation of the eigensolutions of the matrix $\mathbf{S}$ in Eq. (16) may be subject to numerical ill-conditioning, especially when the number of boundary DOFs is large. To overcome this issue, the following $(\mathbf{N}, \mathbf{L})$ eigenproblem method can be considered (Zhong and Williams, 1995; Mencik, 2014):

$$\mathbf{N}\mathbf{w}_j = \mu_j \mathbf{L}\mathbf{w}_j, \tag{24}$$

where

$$\mathbf{L} = \begin{bmatrix} \mathbf{I}_n & \mathbf{0} \\ -\mathbf{D}_{\mathrm{LL}}^{*} & -\mathbf{D}_{\mathrm{LR}}^{*}, \end{bmatrix} \tag{25}$$

$$\mathbf{N} = \begin{bmatrix} \mathbf{0} & \mathbf{I}_n \\ \mathbf{D}_{\mathrm{RL}}^{*} & \mathbf{D}_{\mathrm{RR}}^{*} \end{bmatrix}. \tag{26}$$

In Eq. (24), $\mathbf{w}_j$ are the eigenvectors which are expressed in terms of displacement and velocity potential components, only. The original eigenvectors $\boldsymbol{\phi}_j$ are retrieved as $\boldsymbol{\phi}_j = \mathbf{L}\mathbf{w}_j$. Notice that, when the subsystems are symmetric with respect to their mid-plane, the right-going and left-going wave modes are linked as follows:

$$\mathbf{\Phi} = \mathcal{T}\mathbf{\Phi}^{*}, \tag{27}$$

where

$$\mathcal{T} = \begin{bmatrix} \mathcal{R} & \mathbf{0} \\ \mathbf{0} & -\mathcal{R} \end{bmatrix}. \tag{28}$$

Here, $\mathcal{R}$ is a diagonal symmetry transformation matrix. Eq. (27) provides an analytical means to enforce the coherence between the right-going and left-going wave modes, i.e., the fact that they occur in pairs with the same velocities (Mencik, 2010). Without that, the WFE method may suffer from numerical errors which may be dramatic especially for computing the vibroacoustic responses of periodic systems.

2.3 Forced response computation

Consider a periodic system composed of N subsystems (cf. Figure 1) subject to arbitrary boundary conditions on its left and right boundaries. The vectors of displacements and velocity potentials ($\mathbf{q}^{\mathrm{S}}$ and $\mathbf{q}^{\mathrm{F}}$) over the subsystem boundaries are achieved by considering the following wave mode expansions (Mencik, 2014):

$$\mathbf{q}_{\mathrm{L}}^{(k)} = \mathbf{\Phi}_{\mathrm{q}}\boldsymbol{\mu}^{k-1}\mathbf{Q} + \mathbf{\Phi}_{\mathrm{q}}^{\star}\boldsymbol{\mu}^{N+1-k}\mathbf{Q}^{\star}, \quad k = 1, \ldots, N, \tag{29}$$

$$\mathbf{q}_{\mathrm{R}}^{(k)} = \mathbf{\Phi}_{\mathrm{q}}\boldsymbol{\mu}^{k}\mathbf{Q} + \mathbf{\Phi}_{\mathrm{q}}^{\star}\boldsymbol{\mu}^{N-k}\mathbf{Q}^{\star}, \quad k = 1, \ldots, N, \tag{30}$$

where $\mathbf{Q}$ and $\mathbf{Q}^{\star}$ are $n \times 1$ vectors of wave amplitudes defined at the left and right boundaries of the whole periodic system, respectively. Assume, for the sake of clarity, that those left and right boundaries are subject to two prescribed vectors of displacements/velocity potentials ($\mathbf{q}_0 = \mathbf{q}_{\mathrm{L}}^{(1)}$ and $\mathbf{q}'_0 = \mathbf{q}_{\mathrm{R}}^{(N)}$). More precisely, the vectors $\mathbf{q}_0$ and $\mathbf{q}'_0$ are to be expressed as follows:

$$\mathbf{q}_0 = \begin{pmatrix} \mathbf{q}_0^{\mathrm{S}} \\ \mathbf{q}_0^{\mathrm{F}} \end{pmatrix}, \tag{31}$$

$$\mathbf{q}'_0 = \begin{pmatrix} \mathbf{q}_0^{\mathrm{S}\prime} \\ \mathbf{q}_0^{\mathrm{F}\prime} \end{pmatrix}. \tag{32}$$

Hence, by considering Eqs. (29) and (30), the following well-conditioned matrix equation can be established (Mencik, 2014):

$$\begin{bmatrix} \mathbf{I}_n & \mathbf{\Phi}_{\mathrm{q}}^{-1}\mathbf{\Phi}_{\mathrm{q}}^{\star}\boldsymbol{\mu}^N \\ \mathbf{\Phi}_{\mathrm{q}}^{\star-1}\mathbf{\Phi}_{\mathrm{q}}\boldsymbol{\mu}^N & \mathbf{I}_n \end{bmatrix} \begin{pmatrix} \mathbf{Q} \\ \mathbf{Q}^{\star} \end{pmatrix} = \begin{pmatrix} \mathbf{\Phi}_{\mathrm{q}}^{-1}\mathbf{q}_0 \\ \mathbf{\Phi}_{\mathrm{q}}^{\star-1}\mathbf{q}'_0 \end{pmatrix}. \tag{33}$$

This matrix formulation is of the form $\mathcal{A}\mathcal{Q} = \mathcal{F}$, were $\mathcal{Q}$ is the vector of wave amplitudes for the right-going and left-going wave modes, while $\mathcal{F}$ is the vector of excitations. The computation of the vectors of wave amplitudes follows as $\mathcal{Q} = \mathcal{A}^{-1}\mathcal{F}$; also, the vectors of displacements/velocity potentials and structural/acoustic forces at the boundaries of any subsystem (k) can be simply retrieved from Eqs. (29) and (30).

3 NUMERICAL RESULTS

3.1 Dispersion curves

The elasto-acoustic wave mode propagation in a fluid-filled cylindrical shell is analyzed first. Within the WFE framework, a subsystem is considered as shown in Figure 1, which is meshed with 866 DOFs. The number of DOFs on the left/right cross section is $n = 433$, which is split into $n^{\mathrm{S}} = 192$ DOFs for the structure part and $n^{\mathrm{F}} = 241$ DOFs for the fluid part. In this case, the subsystem does not contain internal DOFs. The geometrical properties of the subsystem are: length $d = 0.005$ m; radius of the cylindrical shell $R^{\mathrm{S}} = 0.05$ m, thickness of the cylindrical shell $h = 0.0025$ m where $h/R^{\mathrm{S}} = 0.05$. Regarding the material properties, the cylindrical shell is made of steel with the following characteristics: Young's modulus $E^{\mathrm{S}} = 2.1 \times 10^{11}$ Pa, density $\rho^{\mathrm{S}} = 7850$ kg/m^3, Poissons ratio $\nu^{\mathrm{S}} = 0.3$ and damping loss factor $\eta^{\mathrm{S}} = 0.01$. Also, the internal fluid is air, with a density of $\rho^{\mathrm{F}} = 1.21$ kg/m^3 and a speed of sound of $c^{\mathrm{F}} = 343$ m/s.

The resulting dispersion curves, i.e., the frequency evolution of the wavenumbers β_j, are presented in Figure 2. The results are compared with the analytical solutions issued from the Donnell-Mushtari theory (see Fuller and Fahy (1982)). Here, the parameters $\beta_j R^{\mathrm{F}}$ are plotted as functions of the non-dimensional frequency $\Omega = \omega R^{\mathrm{F}}/c_L$ where c_L is the phase speed of compressional waves in an equivalent Donnell-Mushtari shell (Fuller and Fahy, 1982). For the sake of clarity, only 7 modes are displayed over a frequency band of $\mathbf{\Omega} = [0.1, 2]$. The

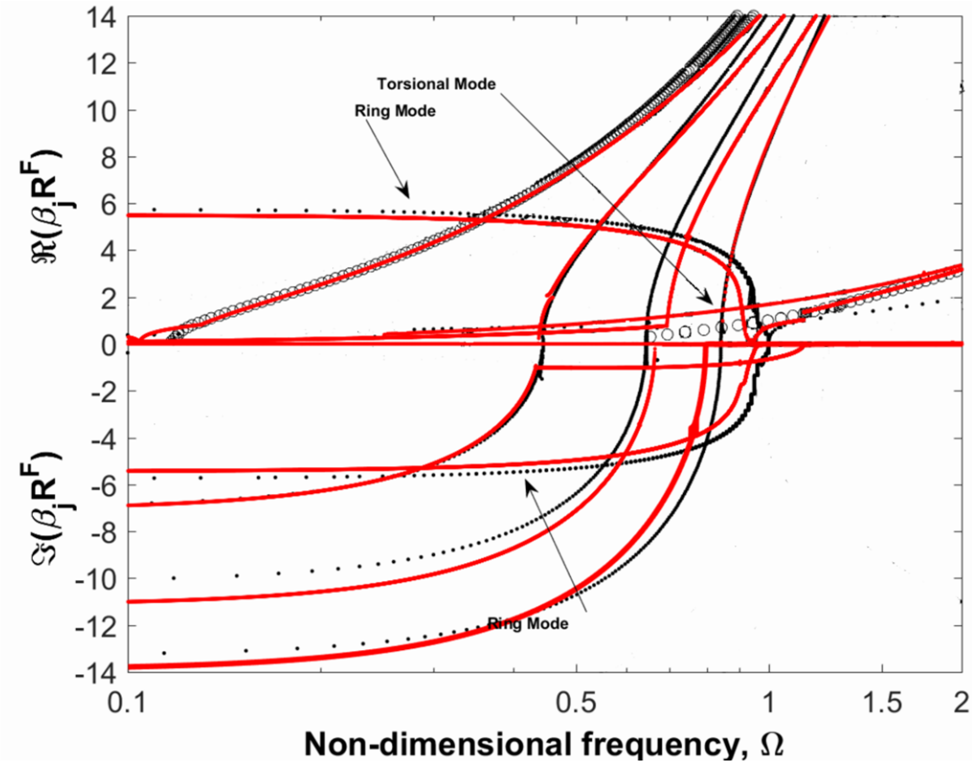

Figure 2: Dispersion curves: WFE solutions (___); analytical solutions for $s = 0$ (. . .); analytical solutions for $s = 1$ (○ ○ ○).

WFE solutions (solid lines) are plotted along with the analytical solutions (dots and circles) that concern the "breathing modes" (zeroth order Bessel function for fluid, $s = 0$) and "beam modes" (first order Bessel function, $s = 1$).

As it can be seen, the numerical results obtained from the WFE method are in good agreement with the analytical theory. In the Donnell-Mushtari shell model, the shearing effects and rotary inertia effects are not taken into account, which is not the case with the proposed WFE method where shell elements that incorporate both membrane and bending motions are considered. Hence, several differences occur between the numerical and analytical solutions, especially at high frequencies where the WFE method works better.

3.2 Forced response

Numerical simulations are carried out to illustrate the efficiency of the WFE method for predicting the vibroacoustic response of fluid-filled shells. Here, a fluid-filled cylindrical shell with a length of 1 m is considered. The material properties and cross-section geometry are the same as those described in Section 3.1. The whole periodic system is modeled by means of $N = 200$ identical subsystems of length $d = 0.005$ m, which are connected along the z-direction. In the present case, the right end of the whole system is clamped (structure part) and subject to zero acoustic pressure (fluid part); also, the left end is clamped (structure part) and subject to a uniform acoustic pressure (fluid part, $\mathbf{p}_0 = 0.001$ Pa $\times \mathbf{1} n^{\mathrm{F}}$). The displacement and pressure solutions are computed with the WFE method and compared with the FE method using MATLAB®. The results are investigated over a non-dimensional frequency band of $\boldsymbol{\Omega} =$

$[0.0055, 0.55]$ which is about $\mathcal{B}_f = [100, 10000]$ Hz. The frequency response function (FRF) that concerns the pressure at the center node of the circular section ($x = 0$, $y = 0$) at the middle of the pipe ($z = 0.5$ m) is plotted as shown in Figure 3.

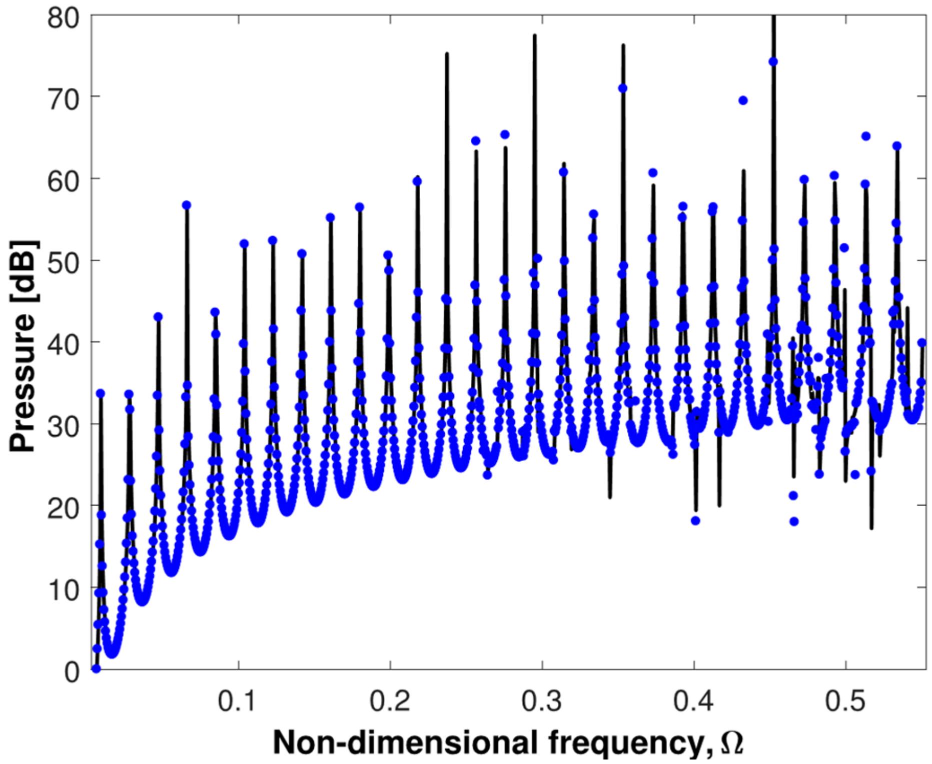

Figure 3: Pressure FRF of the fluid-filled cylindrical shell: FE method (...); WFE method (___).

As it can be seen, the WFE solution perfectly matches the FE one over the whole frequency range. Spurious numerical errors appear at resonances and anti-resonances, which are however only due to frequency sampling and the fact that the fluid is undamped (in other words, high pressure levels occur at resonance frequencies which are not necessarily well captured due to frequency sampling).

The CPU times involved in the WFE and FE methods are highlighted in Table 1. In this case, it takes around 7500 s with the WFE method to compute the FRF of the system over the whole frequency band, against 161,990 s with the FE method. Those simulations have been realized with the same numerical platform, say using MATLAB® and a processor Intel® Core™ i7-3960X. This yields CPU time savings of 95 % in benefit of the WFE method. As it turns out, the WFE method constitutes an efficient/accurate numerical tool for computing the vibroacoustic responses of fluid-filled cylindrical shells.

Table 1: CPU times involved for computing the FRF

Approach used	CPU time [s]	Reduction [%]
FE method	161,990	—
WFE method	7500	95 %

4 CONCLUSION

The WFE method has been applied to analyze the elasto-acoustic wave propagation in fluid-filled cylindrical shells. Emphasis has been placed on improving the FE mesh of the waveguide slice by considering shell elements, instead of 3D linear elements, for modeling the structure parts. In this way, the dispersion diagrams can be computed with accurate precision. Also, the WFE method has been applied to compute the vibroacoustic responses of fluid-filled cylindrical shells of finite length whose left and right boundaries are subject to prescribed displacements/pressures and elastic/acoustic forces. Numerical experiments have been carried out which clearly highlight the computational efficiency of the WFE strategy.

Acknowledgements

The authors are thankful to the Program "Cátedras Francesas na UNICAMP" and Fundação de Apoio à Pesquisa do Estado do Maranhão (FAPEMA) for the financial support.

REFERENCES

Bathe, K.-J. (2015). *Finite element procedures*. Klaus-Jürgen Bathe.

Bhuddi, A., Gobert, M.-L., and Mencik, J.-M. (2015). On the Acoustic Radiation of Axisymmetric Fluid-Filled Pipes Using the Wave Finite Element (WFE) Method. *Journal of Computational Acoustics*, 23:1550011.

Fuller, C. R. and Fahy, F. J. (1982). Characteristics of wave propagation and energy distributions in cylindrical elastic shells filled with fluid. *Journal of Sound and Vibration*, 81(4):501–518.

Gobert, M.-L. and Mencik, J.-M. (2016). A wave finite element-based approach for the prediction of the vibroacoustic behavior of fluid-filled pipes of arbitrary- shaped cross-sections. *International Conference on Noise and Vibration Engineering (ISMA 2016), Leuven, Belgium*.

Kumar, R. (1972). Dispersion of axially Symmetric Waves in Empty and fluid-filled cylindrical Shells. *Acustica*, 27(6):317–329.

Kumar, R. and Stephens, R. W. (1972). Dispersion of flexural waves in circular cylindrical shells. *Proc. R. Soc. Lond.*, A. 329:283–297.

Manconi, E., Mace, B., and Gaziera, R. (2009). Wave finite element analysis of fluid-filled pipes. *Proceedings of NOVEM 2009 "Noise and Vibration: Emerging Methods", Oxford, UK*.

Mencik, J.-M. (2010). On the low- and mid-frequency forced response of elastic systems using wave finite elements with one-dimensional propagation. *Computers and Structures*, 88(11-12):674–689.

Mencik, J.-M. (2014). New advances in the forced response computation of periodic structures using the wave finite element (WFE) method. *Computational Mechanics*, 54(3):789–801.

Mencik, J.-M. and Ichchou, M. N. (2005). Multi-mode propagation and diffusion in structures through finite elements. *European Journal of Mechanics - A/Solids*, 24(5):877–898.

Mencik, J.-M. and Ichchou, M. N. (2007). Wave finite elements in guided elastodynamics with internal fluid. *International Journal of Solids and Structures*, 44:2148–2167.

Morand, H. J.-P. and Ohayon, R. (1992). *Interactions fluids-structures*. Masson.

Quek, S. and Liu, G. (2003). *Finite Element Method: A Practical Course*. Butterworth-Heinemann.

Romero, L. (2007). *Análise de Sensibilidade Vibroacústica de Painéis Aeronáuticos Reforçados*. Master Dissertation, University of Campinas.

Sandberg, G. and Ohayon, R. (2009). *Computational Aspects of Structural Acoustics and Vibration*. CISM International Centre for Mechanical Sciences. Springer Vienna.

Sinha, B. K., Plona, T. J., Kotek, S., and Chang, S. (1992). Axisymmetric wave propagation in fluid-loaded cylindrical shells. I: Theory. *J. Acoust. Soc. Amer.*, 92(2):1132–1143.

Zhong, W. X. and Williams, F. W. (1995). On the direct solution of wave propagation for repetitive structures. *Journal of Sound and Vibration*, 181(3):485–501.

Zienkiewicz, O. and Taylor, R. (2000). *The Finite Element Method: Solid mechanics(second volume)*. Fluid Dynamics. Butterworth-Heinemann.